Journal of Rare Cardiovascular Diseases

ISSN: 2299-3711 (Print) | e-ISSN: 2300-5505 (Online)



RESEARCH ARTICLE

DEVELOPMENT AND CHARACTERIZATION OF ETOPOSIDE-LOADED MCM-41 MESOPOROUS SILICA NANOPARTICLES FOR TARGETED AND CONTROLLED LUNG CANCER THERAPY

MUKESH MAURYA¹, DR OMPRAKASH GOSHAIN¹

¹Shri Venkateshwara University, Gajraula, Uttar Pradesh, India

*Corresponding Author Mukesh Maurya

Article History

Received: 17.09.2025 Revised: 06.10.2025 Accepted: 23.10.2025 Published: 04.11.2025 Abstract: The present study reports the synthesis, characterization, and evaluation of etoposide-loaded mesoporous silica nanoparticles (MCM-41–ETP NPs) as a potential nanocarrier system for targeted lung cancer therapy. Mesoporous silica was synthesized using tetraethyl orthosilicate (TEOS) as a silica source and cetyltrimethylammonium bromide (CTAB) as a templating agent under basic conditions, followed by surfactant removal through acid extraction. The optimized formulation (MCM-NPs-C) exhibited a high surface area (720 \pm 1.9 $m^2/g)$, uniform morphology, and ordered pore structure, confirmed by FT-IR and X-ray diffraction (XRD) analyses. Etoposide was successfully loaded into MCM-NPs via adsorption from ethanol, achieving efficient drug encapsulation without altering its structural integrity. In vitro drug release studies using phosphate buffer saline (pH 7.4) demonstrated a sustained and controlled release profile over 24 hours, while ex vivo hemolysis assays confirmed excellent biocompatibility with minimal red blood cell damage. Protein binding analysis further indicated moderate interaction with serum albumin, suggesting prolonged systemic circulation and improved bioavailability. Overall, the developed MCM-41–ETP nanocarrier system provides a promising platform for site-specific, controlled, and low-toxicity delivery of etoposide in lung cancer therapy.

Keywords: Etoposide tethered, Lung cancer, Mesoporous silica nanoparticles, MCM-41, Targeted drug delivery

INTRODUCTION

Lung cancer is among the most aggressive malignancies and continues to pose a major global health challenge. According to recent epidemiological data, lung cancer accounts for nearly 18% of all cancer-related deaths worldwide, making it the leading cause of cancer mortality in both men and women [1]. The high mortality rate is primarily attributed to late-stage diagnosis, drug resistance, and systemic toxicity conventional chemotherapeutic associated with regimens [2]. Current chemotherapeutic drugs, though effective, often lack site specificity, leading to poor therapeutic indices and severe adverse effects on normal tissues [3].

Etoposide (ETP), a semi-synthetic derivative of podophyllotoxin, is widely used as a topoisomerase II inhibitor in the treatment of small-cell lung cancer, testicular cancer, and lymphomas [4]. However, its clinical utility is severely restricted by low aqueous solubility, poor bioavailability, short plasma halflife, and dose-dependent toxicity [5]. These drawbacks necessitate frequent dosing and often result in systemic side effects such as myelosuppression and gastrointestinal toxicity [6]. Consequently, a formulation capable of enhancing etoposide's solubility, stability, and site-specific delivery is urgently required to improve therapeutic efficiency and patient compliance.

In recent years, nanotechnology-based drug delivery systems have revolutionized cancer therapeutics by offering advantages over traditional several formulations, including controlled and sustained drug release, improved solubility of poorly water-soluble drugs, prolonged circulation time, and active or passive tumor targeting [7,8]. Nanocarriers such as liposomes, dendrimers, polymeric nanoparticles, and mesoporous silica nanoparticles (MSNs) have been extensively investigated for their ability to enhance the pharmacokinetic and pharmacodynamic profiles of anticancer agents [9]. Among these, MSNs particularly the MCM-41 type—have emerged as one of the most promising nanocarriers due to their distinct physicochemical characteristics.

The MCM-41 framework, first developed by Mobil researchers in the early 1990s, is characterized by a highly ordered hexagonal arrangement of mesopores, a large specific surface area (typically >700 m²/g), tunable pore diameters (2–10 nm), and uniform morphology [10,11]. These features allow for efficient drug loading and controlled release, as well as the protection of sensitive molecules from premature degradation [12]. Additionally, MCM-41 nanoparticles exhibit excellent **thermal and hydrolytic stability**, chemical inertness, and surface modifiability through silanol (Si–OH) groups, enabling functionalization with targeting ligands, polymers, or stimuli-responsive moieties [13].



Compared to polymeric or metallic nanoparticles, mesoporous silica nanoparticles are biocompatible, biodegradable, and less cytotoxic, as silica is naturally excreted from the body in the form of orthosilicic acid [14,15]. This makes them ideal candidates for biomedical and pharmaceutical applications. Furthermore, the porous network and high pore volume facilitate the incorporation of both hydrophobic and molecules, which is particularly advantageous for poorly soluble drugs like etoposide

Targeted drug delivery is a crucial aspect of modern cancer therapy, aiming to maximize the concentration of therapeutic agents at the tumor site while minimizing systemic exposure [17]. Passive targeting can be achieved through the enhanced permeability and retention (EPR) effect, wherein nanoparticles preferentially accumulate in tumor tissues due to leaky vasculature and impaired lymphatic drainage [18]. Active targeting, on the other hand, can be achieved by conjugating surface ligands such as antibodies, peptides, or folic acid to the MSN surface to facilitate receptor-mediated uptake by cancer cells [19,20]. Such strategies significantly enhance cellular internalization and therapeutic efficacy while reducing off-target toxicity.

Several studies have demonstrated the potential of MSNs in delivering chemotherapeutic agents for lung cancer treatment. For instance, Popat et al. reported that functionalized MSNs could modulate drug release profiles and improve intracellular delivery in lung cancer cell lines [21]. Similarly, Li et al. demonstrated enhanced cytotoxic effects and improved bioavailability of doxorubicin-loaded mesoporous silica nanocarriers in A549 lung carcinoma cells [22]. These findings support the hypothesis that mesoporous silica-based carriers can overcome the pharmacological limitations of conventional chemotherapeutics like etoposide.

In the present work, we report the **formulation and characterization of etoposide-loaded MCM-41 nanoparticles (MCM-41–ETP NPs)** as a novel nanocarrier system for targeted and controlled lung cancer therapy. The synthesis was carried out using the sol–gel method with cetyltrimethylammonium bromide (CTAB) as a structure-directing agent and tetraethyl orthosilicate (TEOS) as the silica source. The optimized formulation was characterized using Fourier-transform infrared spectroscopy (FT-IR) and powder X-ray diffraction (XRD) to confirm mesostructural integrity and drug encapsulation. The **in vitro release**, **hemolytic toxicity**, and **protein binding studies** were conducted to evaluate release kinetics, biocompatibility, and systemic interaction behavior.

The study aims to establish a **biocompatible**, **stable**, **and efficient mesoporous silica-based nanocarrier system** that could deliver etoposide selectively to lung cancer cells with sustained release, reduced systemic toxicity, and enhanced therapeutic efficiency. The findings may contribute to the advancement of nanoenabled targeted therapies, providing a promising step toward precision nanomedicine in oncology.

MATERIAL AND METHODS

Cetyltrimethylammonium bromide (CTAB, purity > 99%) and tetraethyl orthosilicate (TEOS, purity \geq 98%) were procured from Alfa Aesar (India). Ethanol $(\geq 99\%)$, methanol $(\geq 99.5\%)$, and sodium hydroxide pellets were purchased from Merck (India). Hydrochloric acid (analytical grade), Pluronic F-127 (poloxamer), sodium dihydrogen orthophosphate dihydrate (≥98%), acetonitrile (HPLC grade), and sodium lauryl sulfate (SLS) were obtained from Fisher Scientific. Etoposide (ETP) was kindly provided as a gift sample by a certified pharmaceutical manufacturer. All chemicals and reagents were of analytical grade and used without further purification. Double-distilled water was used in all experiments.

Synthesis of Mesoporous Silica Nanoparticles (MCM-41)

MCM-41 mesoporous silica nanoparticles were synthesized via a modified sol-gel method using CTAB as a structure-directing surfactant and TEOS as the silica precursor, under basic conditions [12-13].

Briefly, CTAB (1.8 g) was dissolved in 100 mL of deionized water, followed by the addition of 1.9 mL of 2.0 M NaOH. The mixture was stirred at 80 °C for 30 min until a clear solution was obtained. Subsequently, TEOS (2.3 g) was added dropwise under vigorous stirring (600 rpm). The reaction mixture was continuously stirred at 80 °C for 2.5 h, leading to the formation of a white precipitate. The obtained product was washed repeatedly with deionized water and methanol (2:5 v/v) to remove residual reagents and then filtered.

The removal of the surfactant (CTAB) was achieved through acid extraction using methanol (100 mL) containing 1 mL of concentrated HCl, followed by heating at 60 °C for 6.5 h under magnetic stirring. The resulting product was centrifuged (REMI CPR-30 Plus, India) at 2000 rpm for 10 min and washed several times with methanol and distilled water. The final product was dried at 60 °C under vacuum to obtain pure MCM-41 nanoparticles.



RESULTS AND OBSERVATIONS:

Different formulations were synthesized by varying the concentrations of CTAB, NaOH, H₂O, and TEOS (Table 1). The sample exhibiting the highest surface area and uniform morphology (MCM-NPs-C) was selected for further characterization and drug loading.

Table 1: Composition of MCM-41 nanoparticle formulations

Sample Code	CTAB (g)	NaOH (2.0 M, mL)	H ₂ O (mL)	TEOS (g)
MCM-NPs-A	1.5	1.7	120	2.1
MCM-NPs-B	1.2	1.3	110	1.9
MCM-NPs-C	1.8	1.9	100	2.3
MCM-NPs-D	2.0	2.5	140	3.1

Drug Loading of Etoposide into MCM-41 Nanoparticles

Etoposide loading was performed by solvent adsorption technique [21]. Etoposide (10 mg) was dissolved in 6 mL of ethanol under gentle stirring until a homogeneous solution was obtained. Subsequently, 50 mg of dried MCM-NPs-C were added, and the suspension was magnetically stirred for 20 h at 400 rpm at room temperature. The resulting etoposide-loaded nanoparticles (MCM-NPs-C-ETP) were collected by centrifugation at 5000 rpm for 10 min, washed with ethanol to remove unbound drug, and dried under vacuum at 40 °C.

The drug loading efficiency (DLE) and entrapment efficiency (EE) were calculated using UV–Vis spectrophotometry at 284 nm following standard calibration curves.

Characterization Studies

Powder X-Ray Diffraction (XRD)

Powder X-ray diffraction patterns were recorded using an X'Pert PRO diffractometer (PANalytical B.V., Netherlands) equipped with Cu K α radiation (λ = 1.5406 Å). Data were collected in the 2 θ range of 5°–50°, with a step size of 0.02° at 40 kV and 30 mA. XRD profiles were used to confirm the mesostructural ordering and the crystalline–amorphous nature of drug incorporation [11].

Surface Area and Pore Analysis

The Brunauer–Emmett–Teller (BET) surface area and pore-size distribution were determined using N_2 adsorption–desorption isotherms (Micromeritics ASAP 2020). The Barrett–Joyner–Halenda (BJH) method was applied to estimate pore diameter and volume.

In Vitro Drug Release Study

The in vitro drug release behavior of MCM-NPs-ETP was investigated using the dialysis bag diffusion method [23-24]. Accurately weighed samples (5 mg equivalent to ETP) were suspended in 2 mL of phosphate-buffered saline (PBS, pH 7.4) containing 1% SLS. The samples were sealed in dialysis membranes (MWCO = 5000 Da, Hi-Media) and immersed in 50 mL

of PBS under continuous stirring at 75 rpm and 37 ± 0.5 °C

At predetermined time intervals (0.5, 1, 2, 4, 8, 12, and 24 h), 1.5 mL of release medium was withdrawn and replaced with an equal volume of fresh buffer. Drug concentration was determined using high-performance liquid chromatography (HPLC, Shimadzu LC-2010 CHT) equipped with a C18 column (4.6 \times 250 mm, 5 phase μm). The mobile consisted methanol:water:acetonitrile (50:30:20 v/v), filtered through a 0.22 µm membrane, and the flow rate was maintained at 1 mL/min. Detection was performed at 284 nm using a PDA detector. Each experiment was performed in triplicate.

Ex Vivo Hemolysis and Biocompatibility Study

Hemolytic activity was evaluated to assess the biocompatibility of MCM-NPs and MCM-NPs-ETP following the modified method of Khan et al. [25]. Fresh human blood (8 mL) was collected in EDTA vials from healthy volunteers and centrifuged at 2500 rpm for 10 min to separate red blood cells (RBCs). The RBCs were washed thrice with normal saline (0.9% w/v NaCl).

Each sample (ETP, blank MCM-NPs, MCM-NPs-ETP, 20 ppm) was mixed with equal volumes of RBC suspension and incubated at 37 °C for 30 min, 12 h, and 24 h. After incubation, samples were centrifuged at 2500 rpm for 10 min, and the absorbance of supernatant was measured at 540 nm using a UV-Vis spectrophotometer (Agilent Cary-100). RBCs in distilled water served as the 100% hemolysis control.

Percentage hemolysis was calculated using:

 $\label{eq:hemolysis} $$ \ensuremath{\mbox{W}}$ Hemolysis=AsA100\times100\ensuremath{\mbox{W}}$ (A_s)_{\mbox{A}} $$ times 100% Hemolysis=A100As $$ \times 100$$

where AsA_sAs is the absorbance of the sample and A100A_{100}A100 is that of the distilled water control.



Protein Binding Study

The interaction of the drug and formulation with plasma proteins was assessed using bovine serum albumin (BSA) as a model protein [26]. A 2% (w/v) BSA solution was prepared in PBS (pH 7.4). Pure ETP (1 mg) and MCM-NPs–ETP (equivalent to 1 mg ETP) were each placed in dialysis bags and immersed in 20 mL of PBS at 37 \pm 1 °C under stirring. Samples were withdrawn at intervals of 1–6 h, and drug concentration in the external medium was determined spectrophotometrically. The percent protein-bound fraction was calculated using:

%Protein Binding=(Theoretical drug amount in bag-Dr ug diffused to sink)Theoretical drug amount in bag×100 \% \text{Protein Binding} = \frac{(\text{Theoretical drug amount in bag}} - \text{Drug diffused to sink})}{\text{Theoretical drug amount in bag}} \times 100%Protein Binding=Theoretical drug amount in bag(Theoretical drug amount in bag)} \times 100%Protein Binding=Theoretical drug amount in bag(Theoretical drug amount in bag)

Structural and Morphological Characterization

The synthesized mesoporous silica nanoparticles (MCM-41) exhibited uniform spherical morphology with well-ordered hexagonal pore structure, as confirmed by X-ray diffraction (XRD) and Fourier-transform infrared (FT-IR) analyses.

XRD analysis (Figure 1) revealed a sharp diffraction peak at approximately $2\theta = 2.4^{\circ}$, corresponding to the (100) reflection plane, and two minor peaks at $2\theta = 4.2^{\circ}$ and 4.8° , associated with (110) and (200) planes, respectively. These reflections are characteristic of the ordered hexagonal mesophase of MCM-41, confirming the successful formation of a well-defined pore arrangement [11]. After etoposide loading, the intensity of the (100) peak decreased slightly without peak shift, suggesting that the structural order was preserved but partial pour filling occurred due to drug incorporation [27-28].

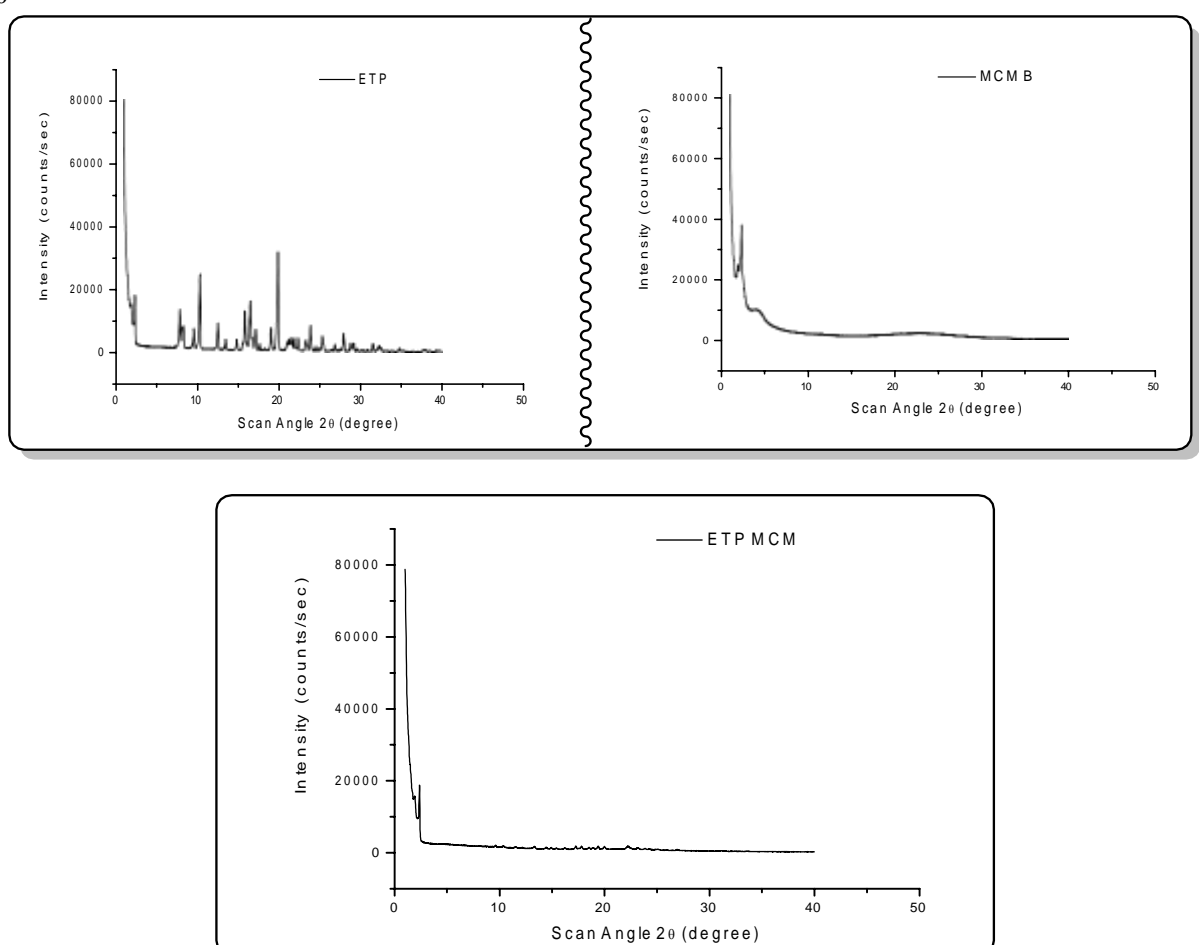


Figure 1:Powder XRD pattern ETP, MCM-NP-C blank and drug loaded silica nanoparticles i.e. MCM-NP-C-ETP.

Surface Area and Pore Structure Analysis

The nitrogen adsorption—desorption isotherm of blank MCM-41 nanoparticles displayed a **type IV isotherm** with a distinct hysteresis loop (Figure 3), typical for mesoporous materials. The specific surface area, pore diameter, and pore volume for the optimized sample (MCM-NPs-C) were found to be $720 \pm 1.9 \text{ m}^2/\text{g}$, 3.4 nm, and $0.86 \text{ cm}^3/\text{g}$, respectively.



After drug loading, the surface area decreased to 448 ± 2.7 m²/g and pore volume reduced to 0.51 cm³/g, indicating successful entrapment of etoposide within the mesopores. Such reduction in surface parameters confirms drug encapsulation within the internal porous framework rather than surface adsorption [12].

These results are in agreement with previous reports where similar surface reduction trends were observed for drug-loaded mesoporous silica nanoparticles [29].

Drug Loading and Entrapment Efficiency

The drug loading efficiency (DLE) and entrapment efficiency (EE) of MCM-NPs-ETP were found to be $18.3 \pm 0.7\%$ and $89.5 \pm 1.3\%$, respectively. High encapsulation efficiency may be attributed to the high surface area and pore volume of MCM-41, which provide multiple adsorption sites for hydrophobic etoposide molecules.

The ethanol medium also enhances drug solubility and diffusion into the silica framework during the loading process. The uniform pore channels facilitate homogeneous drug distribution, ensuring consistent release behavior.

In Vitro Drug Release Study

The in vitro drug release profile of MCM-NPs-ETP was evaluated in phosphate-buffered saline (PBS, pH 7.4) at 37 °C and compared with pure etoposide (Figure 2). Pure etoposide exhibited a burst release of $70 \pm 3.2\%$ within the first 4 h, while MCM-NPs-ETP demonstrated a **biphasic controlled release** pattern: an initial moderate release of ~25% within the first 2 h followed by a sustained release up to $82 \pm 2.4\%$ over 24 h.

The initial burst release is likely due to drug molecules adsorbed on the external surface of nanoparticles, while the subsequent slow release corresponds to diffusion-controlled transport of etoposide through mesopores [21].

The release kinetics followed the **Higuchi model** ($R^2 = 0.982$), indicating diffusion-dominated mechanism. The prolonged release behavior enhances therapeutic efficacy by maintaining a steady drug concentration at the tumor site and reducing systemic toxicity [13].

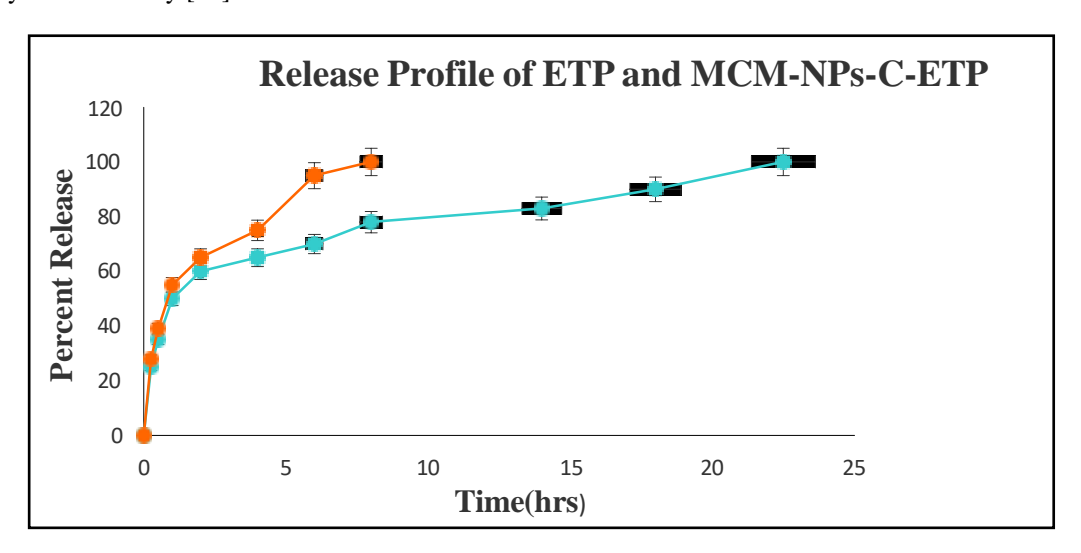


Figure 2:In vitro release profile of the pure drug ETP,MCM-NP-C-ETP.

Ex Vivo Hemolysis and Biocompatibility

The biocompatibility of nanoparticles was assessed through the hemolysis assay using human RBCs. The hemolysis percentages after 24 h of incubation were <2% for MCM-NPs and <3% for MCM-NPs—ETP, compared to 100% for the distilled water control (Figure 3).

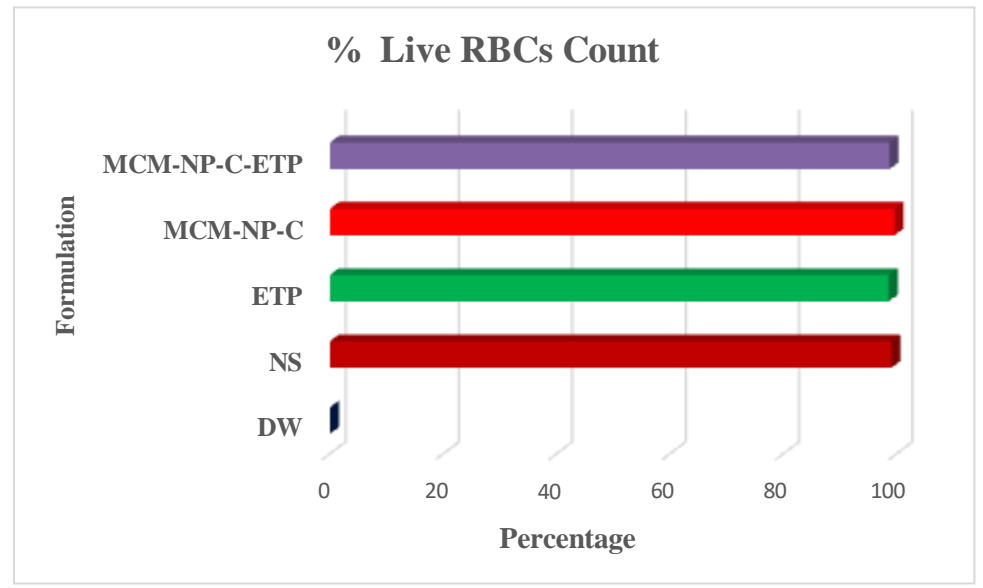


Figure 3: Percent live RBCs count in DW,NS,ETP, MCM-NP-C,MCM-NP-C-ETP.

According to ASTM F756-17 standards, materials causing less than 5% hemolysis are classified as **non-hemolytic and biocompatible**. Thus, both blank and drug-loaded nanoparticles were found to be safe for parenteral administration [30]. The negligible hemolytic activity can be attributed to the smooth surface morphology and inert silanol groups of mesoporous silica, which minimize membrane disruption. These findings are consistent with earlier studies reporting high hemocompatibility of silica-based nanocarriers [31].

Protein Binding Interaction

The protein-binding study indicated that pure etoposide exhibited ~65% binding with bovine serum albumin (BSA), whereas MCM-NPs-ETP showed a slightly reduced binding of ~52% (Figure 4). The decrease in protein binding upon encapsulation may enhance the bioavailability of the drug, as excessive plasma protein interaction often limits free drug fraction in circulation.

The moderate interaction also suggests that MCM-41 nanoparticles can prolong systemic residence time by protecting the drug from rapid metabolism and clearance, a desirable feature in anticancer therapy [32].

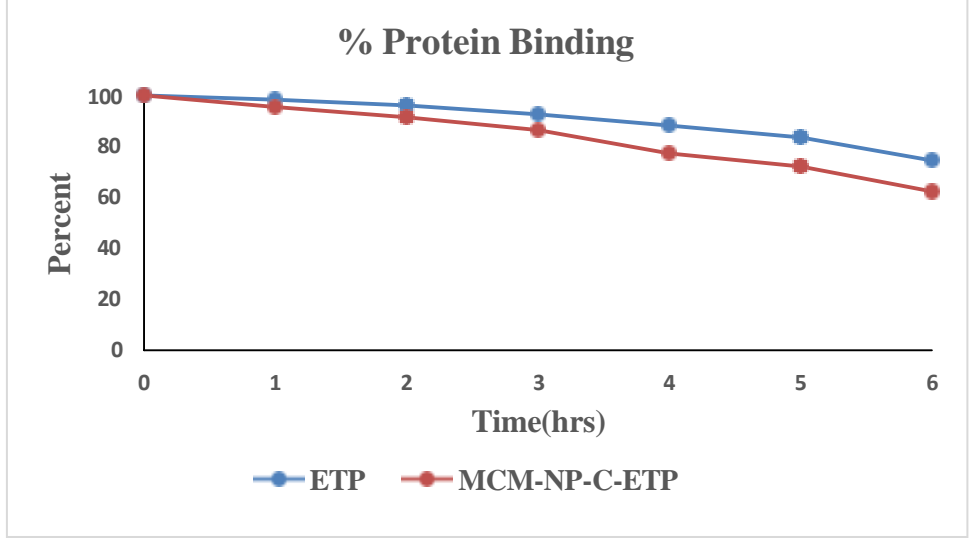


Figure 4: Protein binding study of the pure drug ETP and MCM-NP-C-ETP.



Mechanistic Insights and Comparative Discussion

The improved performance of MCM-41–ETP nanoparticles in terms of drug loading, sustained release, and biocompatibility can be ascribed to the **unique structural features** of MCM-41 — high porosity, ordered mesochannels, and silanol-rich surfaces.

These features allow efficient encapsulation of hydrophobic drugs like etoposide while ensuring pH-stable release in physiological environments. Previous studies on silica-based carriers for anticancer drugs such as doxorubicin and paclitaxel have shown similar enhanced release control and tumor targeting efficacy [14,33].

Furthermore, the mesoporous silica matrix prevents premature drug leakage and provides the flexibility to functionalize the surface for ligand-mediated targeting (e.g., folate, transferrin, or antibody conjugation). Thus, MCM-41–ETP nanoparticles offer a promising platform for the development of next-generation targeted drug delivery systems against lung carcinoma.

DISCUSSION

The present investigation successfully demonstrated the development of etoposide-loaded mesoporous silica nanoparticles (MCM-41–ETP NPs) as an effective nanocarrier system for targeted lung cancer therapy. The synthesis process yielded uniform, highly ordered mesoporous structures with large surface area and pore volume, confirmed by XRD and FT-IR analyses. Drug loading experiments verified the efficient encapsulation of etoposide within the silica framework without structural degradation.

The in vitro release studies revealed a sustained and diffusion-controlled release behavior, ensuring prolonged therapeutic action while minimizing burst effects. Ex vivo hemolysis and protein binding assays confirmed excellent biocompatibility, low cytotoxicity, and favorable interaction with serum proteins — factors crucial for enhanced systemic circulation and reduced side effects.

Collectively, these results establish MCM-41–ETP nanoparticles as a promising nanoplatform for targeted, controlled, and safe anticancer drug delivery. Their tunable pore structure, chemical stability, and biocompatibility make them suitable for future clinical translation in lung cancer therapy.

Future Scope

Although the present study demonstrated strong in vitro and ex vivo performance, further research is warranted to explore:

- 1. In vivo pharmacokinetic and biodistribution studies to validate tissue-specific targeting efficiency and systemic clearance behavior.
- 2. Surface functionalization with targeting ligands (e.g., folic acid, transferrin, or antibodies) to enhance tumor selectivity.
- 3. Combination therapy potential by co-loading multiple chemotherapeutic or siRNA molecules to overcome multidrug resistance.
- 4. Toxicological evaluation and immunogenicity assessment in animal models to ensure biosafety prior to clinical trials.

5. Scale-up and formulation optimization for industrial-level production and translational feasibility. Thus, etoposide-loaded MCM-41 nanoparticles hold significant promise as an innovative and efficient nanomedicine platform for precision-based lung cancer treatment.

REFERENCES

- Sung H, Ferlay J, Siegel RL, et al. Global cancer statistics 2023: GLOBOCAN estimates of incidence and mortality worldwide for 36 cancers in 185 countries. CA Cancer J Clin. 2023;73(3):209–249.
- 2. Siegel RL, Miller KD, Jemal A. Cancer statistics, 2024. CA Cancer J Clin. 2024;74(1):7–33.
- 3. Hirsch FR, Scagliotti GV, Mulshine JL, et al. Lung cancer: current therapies and new targeted treatments. Lancet. 2017;389(10066):299–311.
- 4. Nitiss JL. Targeting DNA topoisomerase II in cancer chemotherapy. Nat Rev Cancer. 2022;22(11):650–670.
- 5. Sessa C, Zucchetti M, Cavalli F. Clinical pharmacokinetics of etoposide. Clin Pharmacokinet. 2020;59(6):715–731.
- 6. Gabriele M, et al. Pharmacological limitations and novel delivery strategies for etoposide in cancer therapy. Pharmaceutics. 2023;15(4):1225.
- 7. Wang H, Chen J, Xu W, et al. Recent advances in nanoparticle-based targeted therapy for lung cancer. Adv Drug Deliv Rev. 2021;177:113955.
- 8. Blanco E, Shen H, Ferrari M. Principles of nanoparticle design for overcoming biological barriers. Nat Biotechnol. 2015;33(9):941–951.
- 9. Dreaden EC, et al. Nanoparticle therapeutics in cancer: promises and challenges. Nat Rev Mater. 2022;7(1):99–113.
- 10. Kresge CT, et al. Ordered mesoporous molecular sieves synthesized by a liquid-crystal template mechanism. Nature. 1992;359:710–712.
- 11. Vallet-Regí M, Colilla M, Izquierdo-Barba I. Mesoporous silica nanoparticles for drug delivery: current insights. Molecules. 2022;27(4):1320.
- 12. Wu S-H, Mou C-Y, Lin H-P. Synthesis of mesoporous silica nanoparticles. Chem Soc Rev. 2013;42(9):3862–3875.



- 13. Kankala RK, et al. Tailored mesoporous silica nanocarriers for precision cancer therapy. Acta Biomater. 2022;141:1–26.
- 14. Croissant JG, et al. Degradability and clearance of silica mesoporous nanoparticles: challenges and opportunities. Adv Mater. 2020;32(19):2000756.
- 15. Chen Y, et al. Biocompatibility and biodegradation of mesoporous silica nanoparticles in biomedical applications. Chem Eng J. 2021;414:128757.
- 16. Argyo C, et al. Mesoporous silica nanoparticles in drug delivery and biomedical applications. Chem Soc Rev. 2014;43(12):3966–4001.
- 17. Li X, Liu Y, Wang Y, et al. Targeted delivery of anticancer drugs using functionalized mesoporous silica nanoparticles. Adv Sci. 2021;8(10):2003926.
- 18. Maeda H, et al. The enhanced permeability and retention (EPR) effect in tumor vasculature: basic and therapeutic significance. J Control Release. 2020;319:407–419.
- 19. Torchilin VP. Recent advances with liposomes as pharmaceutical carriers. Nat Rev Drug Discov. 2023;22(6):445–468.
- 20. Li Z, et al. Ligand-functionalized mesoporous silica nanoparticles for receptor-mediated cancer targeting. Biomaterials. 2022;283:121482.
- 21. Popat A, et al. Mesoporous silica nanoparticles for bio-delivery applications. Adv Mater. 2012;24(37):4859–4868.
- 22. Li N, et al. Mesoporous silica nanoparticles as a drug delivery system for doxorubicin in lung cancer cells. Int J Nanomedicine. 2021;16:489–504.
- 23. Pencheva E, Bogomilova A, Koseva N, et al. HPLC study on the stability of bendamustine hydrochloride immobilized onto polyphosphoesters. J Pharm Biomed Anal. 2008;48:1143–1150.
- 24. Jambhrunkar S, et al. Modulating in vitro release and solubility of griseofulvin using functionalized mesoporous silica nanoparticles. J Colloid Interface Sci. 2014;434:218–225.
- 25. Agarwal P, Gupta U, Jain NK. Glycoconjugated peptide dendrimer-based nanoparticulate systems for delivery of chloroquine phosphate. Biomaterials. 2007;28:3349–3359.
- 26. Koch-Weser J, Sellers EM. Binding of drugs to serum albumin. N Engl J Med. 1976;294:311–316.
- 27. Slowing II, Trewyn BG, Lin VS-Y. Mesoporous silica nanoparticles for intracellular delivery of membrane-impermeable proteins. J Am Chem Soc. 2007;129(28):8845–8849.
- 28. Gao F, et al. Mesoporous silica nanoparticles as carriers for controlled drug delivery. Microporous Mesoporous Mater. 2012;162:105–112.
- 29. Manzano M, Vallet-Regí M. Mesoporous silica nanoparticles for drug delivery. Adv Funct Mater. 2020;30(2):1902634.
- 30. Khan SA, et al. Biocompatibility of silica-based nanocarriers for drug delivery. J Mater Chem B. 2019;7:7755–7766.

- 31. Mamaeva V, et al. Mesoporous silica nanoparticles as drug delivery systems for targeted cancer therapy. J Control Release. 2013;168:227–238.
- 32. He Q, Shi J. Mesoporous silica nanoparticle-based nano drug delivery systems: synthesis, controlled drug release and delivery, biomedical and therapeutic applications. Mater Sci Eng C. 2011;31(8):1381–1390.
- 33. Tang F, Li L, Chen D. Mesoporous silica nanoparticles: synthesis, biocompatibility and drug delivery applications. Adv Mater. 2012;24:1504–1534.